Abstract. The size-selective synthesis of hexagonal Sb_2Te_3 nanoplates by thermal decomposition of the *single source precursor* bis(diethylstibino)telluride $(Et_2Sb)_2Te$ is described for the first time. The role of the thermolysis temperature and the concentration of the capping agent (PVP*) on the growth of the nanoplates was investigated. The thermal properties of $(Et_2Sb)_2Te$ were investigated by differential scanning calorimetry (DSC) and the resulting Sb_2Te_3 nanoplates were characterized by XRD, SEM, TEM, EDX and SAED. Moreover, electrical conductivity and Seebeck coefficient and thermal conductivity of the nanoplates were determined, clearly proving the enhanced thermoelectric properties of nanosized antimony telluride.

Stephan Schulz,* Stefan Heimann, Jochen Friedrich, Markus Engenhorst, Gabi Schierning, Wilfried Assenmacher

Chem. Mater. **2012**, *24*, pp

Synthesis of Hexagonal Sb_2Te_3 Nanoplates by Thermal Decomposition of the *Single Source Precursor* $(Et_2Sb)_2Te$.

The size- and shape-selective synthesis of hexagonal Sb_2Te_3 nanoplates by thermal decomposition of a *single source precursor* in the presence of suitable capping agents is described. The resulting nanoplates show enhanced thermoelectric properties.

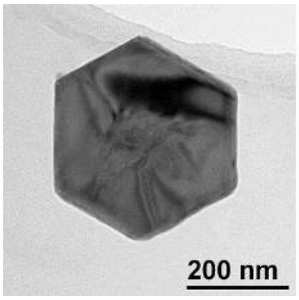

Synthesis of Hexagonal Sb_2Te_3 Nanoplates by Thermal Decomposition of the *Single Source Precursor* $(Et_2Sb)_2Te$.

Stephan Schulz,[a]* Stefan Heimann,[a] Jochen Friedrich,[a] Markus Engenhorst,[b] Gabi Schierning,[b] Wilfried Assenmacher[c]

[a] Institute of Inorganic Chemistry and Center for Nanointegration Duisburg-Essen (CeNIDE), University of Duisburg-Essen, Universitätsstr. 5-7, D-45117 Essen, Germany. [b] Faculty of Engineering and Center for Nanointegration Duisburg-Essen (CeNIDE), University of Duisburg-Essen, Bismarckstr. 81, D 47057 Duisburg, Germany. [c] Institute of Inorganic Chemistry, University of Bonn, Römerstr. 164, D-53117 Bonn, Germany.

KEYWORDS. Nanostructures – Thermal decomposition – Antimony telluride – Nanoplates – Thermoelectric Materials

Supporting Information Placeholder

ABSTRACT: The size-selective synthesis of hexagonal Sb_2Te_3 nanoplates by thermal decomposition of the *single source precursor* bis(diethylstibino)telluride $(Et_2Sb)_2Te$ is described for the first time. The role of the thermolysis temperature and the concentration of the capping agent (PVP*) on the growth of the nanoplates was investigated. The thermal properties of $(Et_2Sb)_2Te$ were investigated by differential scanning calorimetry (DSC) and the resulting Sb_2Te_3 nanoplates were characterized by XRD, SEM, TEM, EDX and SAED. Moreover, electrical conductivity and Seebeck coefficient and thermal conductivity of the nanoplates were determined, clearly proving the enhanced thermoelectric properties of nanosized antimony telluride.

Introduction

Nanosized materials with at least one dimension between 1 and 100 nm, which often exhibit different electrical and optical properties compared to their bulk phases,[1,2] show promising technical applications in nano- and optoelectronic devices.[3-5] Therefore, wet chemical approaches for the size- and form-selective synthesis of nanoparticles such as nanowires[6] and nanotubes[7] have been studied over the last decade,[8] in particular the polyol process and the thermal decomposition of molecular metal organic precursors.[9] Anisotropic growth was achieved by addition of specific surfactants, that preferentially bind to suitable crystal faces of the growing particles.[10,11] The inherent anisotropy of the crystal structure or crystal surface reactivity forces the low-dimensional growth.[12,13]

Tailored nanostructures offer a great potential for energy applications, for instance in the field of thermoelectric energy conversion. Thermoelectric materials convert heat fluxes into useable electric energy by exploiting the Seebeck effect, and could play a major role in waste heat harvesting provided that the conversion efficiency is sufficient. The thermal-to-electrical energy conversion efficiency is directly related to the materials' specific dimensionless figure of merit zT. Theoretical predictions[14,15] and experimental findings[16,17] demonstrated that the figure of merit, which is expressed as $zT = (\alpha^2\sigma/\kappa)T$, where T is the temperature in Kelvin, α is the Seebeck coefficient, σ is the specific electrical conductivity and κ is the thermal conductivity, can be significantly improved in nanoscale thermoelectric (TE) materials. The reason is that the electronic and thermal transport properties can be decoupled by nanostructuring which is otherwise very difficult to achieve. As a consequence, the synthesis of TE nanostructures was studied in detail. Several nanostructured TE materials with different morphologies and sizes were synthesized by various methods, including template methods,[18,19] chemical deposition,[20] and solvothermal or hydrothermal processes.[21-24]

Antimony telluride (Sb_2Te_3), which belongs to the layered semiconductors with tetradymite structure, and its doped derivatives are promising candidates for near room-temperature TE applications due to their promising zT values in the temperature range of 300-500 K.[25,26] As a consequence, bulk Sb_2Te_3 finds technical applications in minipower-generation systems and microcoolers, charge coupled device (CCD) technology, and infrared detectors.[27-30] Further figure of merit enhancement is expected by nanostructuring these semiconductors[31-33] due to increased interface scattering of phonons which reduces the thermal conductivity.[34-36] By adjusting the size of the nanostructure such that it is smaller than the phonon mean free path but considerably larger than the electron mean free path, the fraction σ/κ can be optimized.

Antimony telluride nanostructures with well defined morphologies can be synthesized by gas phase processes such as chemical vapor deposition[37-39] and vapor transport growth,[40] as well as in solution by hydrothermal processes[23,41-46] and by microwave heating.[47] As-formed Sb_2Te_3 nanoparticles typically showed enhanced Seebeck coefficients and reduced thermal conductivity compared to bulk Sb_2Te_3.[40,48,49,50] In addition, compound materials of antimony and tellurium are a new class of thermoelectric materials, and very recently, an enhanced thermoelectric power factor (~2 μW/(cm·K^2)) was reported for Ag_xTe_y-Sb_2Te_3 heterostructured films.[51]

We report herein on the shape-selective synthesis of almost monodisperse hexagonal Sb_2Te_3 nanoplates by thermal decomposition of the *single source precursor* $(Et_2Sb)_2Te$ **1**, which is a stable liquid at ambient temperature. To the best of our knowledge, this is the first report on the use of a *single source precursor* in the solution-based synthesis of Sb_2Te_3 nanoparticles. The use of this molecular precursor, whose intrinsic chemical composition allows the synthesis of the desired material without the use of any other reagent is quite interesting, since the workup of the resulting material is quite easy. The thermal properties of **1**, which was prepared in almost quantitative yield by insertion reaction of elemental Te into the Sb-Sb bond of tetraethyldistibine Et_4Sb_2, were investigated by DSC. The distinctive role of different solvents and capping agents on the size- and shape-selective growth of antimony telluride nanoparticles was investigated in detail. The resulting Sb_2Te_3 nanoparticles were characterized by XRD, SEM, TEM, and EDX. Moreover, thermal and electrical conductivity as well as Seebeck coefficient of a cold pressed pellet prepared from the Sb_2Te_3 nanoplates were determined.

Experimental Section

Materials. Tellurium, TOPO, dodecylamine and PVP* (CAS 136445-69-7) were used as received. 1,3-diisopropylbenzene (DIPB) was purchased from Fluka, carefully dried over Na/K alloy and degassed prior to use. Et_4Sb_2 was prepared according to a literature method.[52] All synthetic steps were performed in a glovebox under Ar atmosphere.

Synthesis of $(Et_2Sb)_2Te$ (1). $(Et_2Sb)_2Te$ was prepared according to a slightly modified literature method.[53] Elemental tellurium (1.30 g; 10 mmol) was added to a solution of tetraethyldistibine Et_4Sb_2 (1.80 g; 5 mmol) in 5 mL of pentane and the resulting suspension was stirred at ambient temperature for 72 h. Unreacted tellurium was removed by filtration and **1** was isolated after workup of the pentane solution in almost quantitative yield.

^{1}H NMR (C_6D_6, 25 °C, 300 MHz): δ = 1.31 (t, $^3J_{HH}$ = 7.8 Hz, 12H, CH_3), 1.54-1.66 (dq, $^2J_{HH}$ = 12.3 Hz, $^3J_{HH}$ = 8.0 Hz, 4H, CH_2), 1.72-1.85 (dq, $^2J_{HH}$ = 12.3 Hz, $^3J_{HH}$ = 8.0 Hz, 4H, CH_2). ^{13}C NMR (C_6D_6, 25 °C, 300 MHz): δ = 7.8 (CH_2), 13.7 (CH_3).

Synthesis of hexagonal Sb_2Te_3 nanoplates. 0.20 g $(Et_2Sb)_2Te$ was added to a freshly prepared solution of 0.125 g PVP* in 10 mL of DIPB at ambient temperature. The solution was then heated to 180 °C for 10 h, yielding a black suspension, from which a very small amount of an insoluble precipitate was isolated by centrifugation. The remaining black solution, which is stable for at least one week under Ar atmosphere, contained colloidal-dissolved hexagonal Sb_2Te_3 nanoplates, which were isolated after addition of methanol and centrifugation. Additional PVP* was removed by repeated (2 - 3 times) redispersion ($CHCl_3$), precipitation (MeOH) and centrifugation under Ar atmosphere in the glovebox.

SEM Analysis. SEM studies were carried out on an ESEM Quanta 400 FEG or a Jeol JSM 6510 equipped with an energy dispersive X-ray spectroscopy (EDX) device (Bruker Quantax 400). A cross section sample of the Sb_2Te_3 pellet was prepared by use of a Jeol Cross-Section Polisher (IB-09010CP).

TEM Analysis. TEM studies were performed on a Philips CM30T (LaB_6-cathode) operated at 250 keV and equipped with an EDX-detector (ThermoScientific Nanotrace NSS) for EDX-analysis. The samples were prepared on perforated carbon foils without further grinding.

X-ray Analysis. XRD patterns were obtained using a Bruker D8 Advance powder diffractometer with Cu K_α radiation (λ: 1.5418 Å).

Thermoelectric properties. The as-prepared nanostructures were cold-pressed to two pellets of 5 mm and 13 mm diameter (10 min, 600 MPa). Transport characterization was performed in a temperature regime from room temperature (RT) to 200 °C and always along the pressing direction of the respective pellets. Thermal diffusivity, λ, of the pellet with 13 mm diameter was measured using an *LFA 457 Microflash* from *NETZSCH-Gerätebau GmbH*. The heat capacity, c_p, was calculated from ref. 53.[54] The density, ρ, was measured by exploiting the Archimedes principle. Thermal conductivity was calculated from $\kappa = \lambda \cdot \rho \cdot c_p$. Seebeck coefficient and electrical conductivity were measured using the pellet with 5 mm diameter in a commercial system *ZEM-3* by *Ulvac Technologies, Inc.* under Helium atmosphere at 100 mbar. The power factor, $\alpha^2\sigma$, and the thermoelectric figure of merit, *z*T, were calculated from the single measurements which were obtained using different pellets but the same transport direction. Additionally, some powder was exposed to a rapid thermal annealing (30 sec, 350 °C, N_2), cold-pressed, and subsequently characterized as described above. Both, thermal and electrical transport measurements were repeated several times in order to exclude in-situ annealing effects during the measurements. After three runs, no change in the temperature dependant transport coefficients was seen any more. Since thermal conductivity and electronic properties were not measured at exactly the same temperature in the case of the native sample, we extrapolated the values in between the data points and calculated *z*T accordingly.

Results and Discussion

$(Et_2Sb)_2Te$ **1** was prepared by reaction of elemental tellurium with tetraethyldistibine Et_4Sb_2 in pentane at ambient temperature, which gave **1** in almost quantitative yield after 72 h.

$$Et_4Sb_2 + Te \xrightarrow{25\ °C} (Et_2Sb)_2Te$$

Scheme 1. Synthesis of $(Et_2Sb)_2Te$ **1**.

These type of complexes containing the heavy elements of group 15 (Sb, Bi) and group 16 (Se, Te) are known for more than thirty years.[53,55,56] They are typically thermally labile com-

plexes which tend to decompose upon heating with formation of the antimony or bismuth chalcogenide M_2E_3 (M = Sb, Bi; E = Se, Te) and the corresponding trialkylstibine and –bismuthine R_3E, respectively, as shown in scheme 2. Surprisingly, this decomposition reaction to best of our knowledge was never used for the size- and shape-selective growth of group 15/16 nanoparticles.

$$3\ (Et_2Sb)_2Te \xrightarrow{180\ °C} Sb_2Te_3 + 4\ SbEt_3$$

Scheme 2. Thermally induced decomposition reaction of **1**.

According to a DSC study, **1** starts to decompose at about 160 °C with subsequent formation of $SbEt_3$ as was previously confirmed by ^{1}H NMR spectroscopy. The decomposition of **1** is finished at 200 °C, whereas the as-formed $SbEt_3$ decomposes between 300 and 340 °C (Fig. 1a). Moreover, the DSC curve shows an endothermic peak at 345 °C, whose origin is not clear yet. The melting point of bulk Sb_2Te_3 is significantly higher (620 °C),[57] so it is questionable if this peak points to a melting of the as-formed Sb_2Te_3 nanoparticles. However, previously prepared 200 nm sized Sb_2Te_3 nanoplates were reported to have a melting point of 419.7 °C.[48] In contrast, a DSC experiment (Fig. 1b) of our isolated 300 nm sized Sb_2Te_3 nanoplates showed an endothermic peak at 612 °C, which corresponds very well with the melting point of the bulk phase, as well as an endothermic peak at 407 °C, which agrees fairly with that reported by Zhang et al. (419.7 °C).[48]

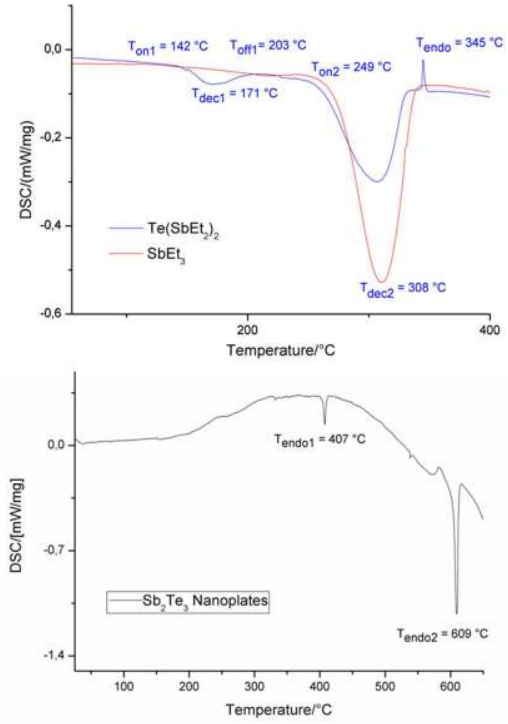

Figure 1. a) DSC of **1** (blue curve) proving the decomposition to start at about 160 °C with formation of Sb_2Te_3 and $SbEt_3$, which decomposes at 270 °C. Freshly prepared $SbEt_3$ shows the same thermal decomposition temperature (red curve). b) DSC study of isolated Sb_2Te_3 nanoplates.

These findings were experimentally verified by a thermal decomposition of 0.2 g **1** in a closed glass ampoule at 170 °C, yielding a black precipitate and a colorless liquid. The solid was identified as Sb_2Te_3 by XRD and the liquid as $SbEt_3$ by ^{1}H NMR spectroscopy. SEM studies showed the formation of highly aggregated Sb_2Te_3 nanoplates (Fig. 2).

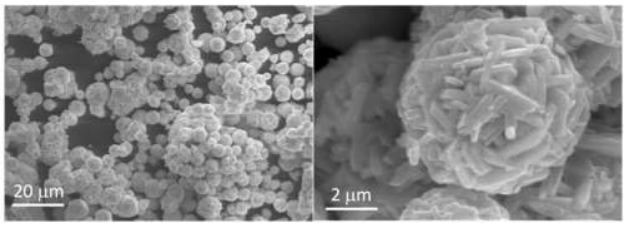

Figure 2. SEM photographs of agglomerated Sb_2Te_3 nanoplates obtained from thermolysis of **1** in a closed glass ampoule.

In order to reduce the agglomeration rate, the thermolysis reaction of **1** was performed at 170 °C in DIPP in the presence of PVP*. A small amount of insoluble black solid was formed, which was isolated by centrifugation at 2000 RPM. After addition of 10 mL of MeOH, a black solid precipitated, which was isolated by centrifugation. The solid was redispersed in $CHCl_3$ and purified by repeated (3x) addition of methanol, centrifugation and redispersion.

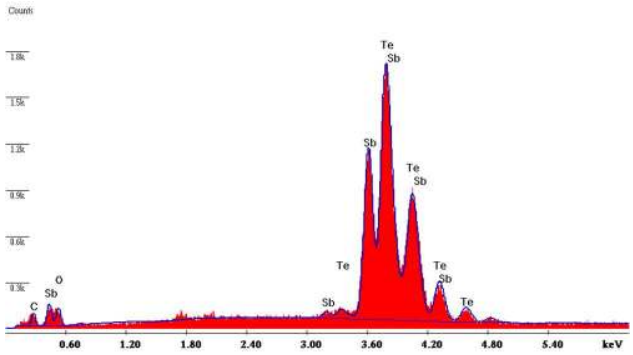

Figure 3. EDX spectrum of Sb_2Te_3 nanoplates formed at 170 °C.

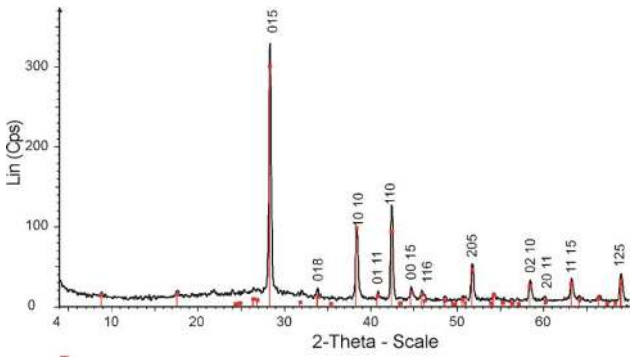

Figure 4. 2-theta XRD pattern of the Sb_2Te_3 nanoplates; the most intense peaks are labeled.

EDX (Fig. 3) showed the formation of a slightly tellurium-deficient Sb_2Te_3 phase, whereas XRD studies (Fig. 4) proved the

presence of pure, crystalline Sb_2Te_3 nanoplates. All the reflection peaks with a significant intensity in the X-ray diffractogram can be indexed on the basis of the structure of rhombohedral Sb_2Te_3.

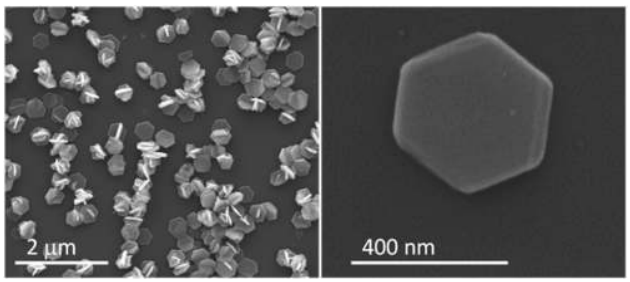

Figure 5. SEM photographs of Sb_2Te_3 nanoplates formed in DIPP/PVP* solution at 170 °C.

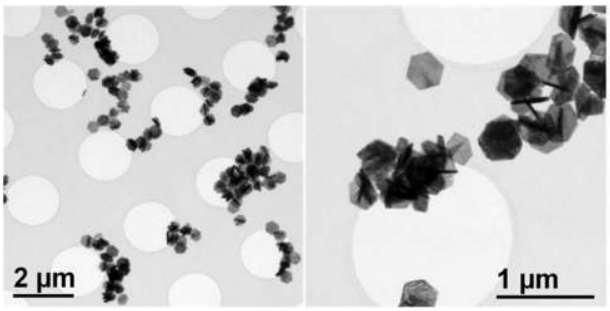

Figure 6. TEM micrographs of Sb_2Te_3 nanoplates formed in DIPP/PVP* solution at 170 °C.

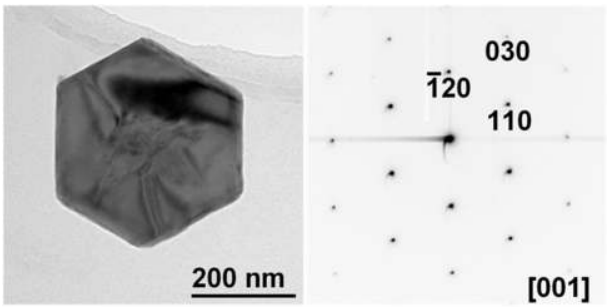

Figure 7. TEM micrograph of a single Sb_2Te_3 nanoplate formed in DIPP/PVP* solution at 170 °C and corresponding inverted SAED pattern in [001] orientation.

SEM analysis clearly proved that these particles are hexagonal, almost monodisperse Sb_2Te_3 nanoplates of roughly 400 nm in diameter and 35 nm in thickness (Fig. 5) as was confirmed by TEM studies (Fig. 6). The SAED (Figure 7) studies clearly revealed the formation of crystalline Sb_2Te_3 particles.

Hexagonal Sb_2Te_3 nanoplates with 100–200 nm in diameter were previously synthesized on glass substrates by an aerosol-assisted chemical vapor deposition process (AACVD) at significantly higher reaction temperatures (375 to 475 °C) using the *single-source precursor* $Sb[(TeP\textit{i}\text{-}Pr_2)_2N]_3$.[58] Moreover, Sb_2Te_3 nanoplates were obtained by a solvothermal route by reaction of $SbCl_3$, elemental Te powder and $NaBH_4$ in the presence of CTAB at 200 °C.[23] However, the shape of as-formed Sb_2Te_3 nanoplates was rather heterogenic, with an edge-length ranging from 200 nm to 2 µm and a thickness of several tens of nanometers. Moreover, these hexagonal Sb_2Te_3 nanoplates were transformed into nanorings driven by growth temperature in a simple solvothermal process.[59] In addition, their transformation into porous Te plates by hydrothermal treatment at 180 °C in the presence of a trace amount of oxygen was described.[60] Very recently, *Chen et al.* reported on the glucose-assisted solvothermal synthesis of uniform Sb_2Te_3 nanoplates with a thickness of roughly 40 nm at 140 °C.[61]

The formation of hexagonal Bi_2Te_3 nanoplates, which were prepared by a high-temperature organic solution approach,[62] was explained by the anisotropic structure of Bi_2Te_3, which forms a layered structure that is stacked along the *c*-axis. The formation of nanoplate seeds was proposed as the initial step on the formation of Bi_2Te_3 nanoplates,[63] since these seeds were expected to exhibit a higher growth rate along the planes perpendicular to the c-axis, resulting in the formation of uniform nanoplates. Stabilizing agents capped on the surfaces of Bi_2Te_3 nanocrystals may further increase the growth rate of these planes. In addition, temperature was identified as the key factor for the controlled growth of uniform Bi_2Te_3 nanoplates. Low reaction temperature yielded thin, but rather irregular nanoplates, whereas higher reaction temperatures resulted in the formation of thick, but almost monodisperse nanoplates.

In our experiments, the formation of hexagonal Sb_2Te_3 nanoplates was almost independent from the reaction temperature, which was varied from 160 to 200 °, whereas the concentration of the capping agent strongly influences the particle size. With increasing PVP* concentration (3, 10, 20 and 50 weight percentage), the average diameter of the hexagons decreased from about 500 nm to roughly 200 nm.

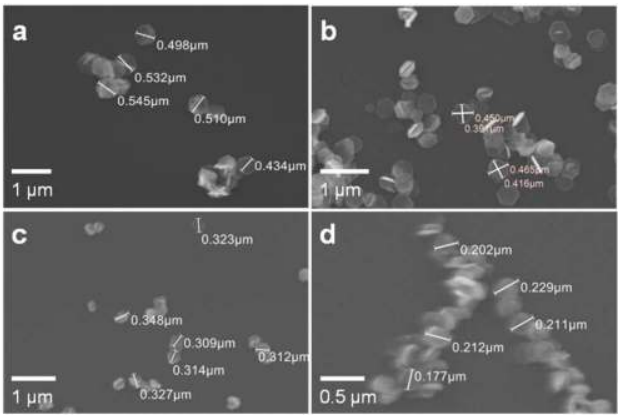

Figure 8. SEM photographs of Sb_2Te_3 nanoplates obtained with PVP* concentrations of 3 (a), 10 (b) , 20 (c) and 50 (d) weight % at 170 °C.

The growth mechanism of our Sb_2Te_3 nanoplates also seems to be strongly influenced by the the crystal structure of rhombohedral Sb_2Te_3, which adopts a layered anisotropic lattice structure with infinite -Te_1-Sb-Te_2-Sb-Te_1-chains along the c-axis direction and *van der Waals* bonds between adjacent Te_1 layers.[48] Since the free energy of a broken covalent bond is higher

than that of a dangling *van der Waals* bond, the growth process along the top–bottom crystalline plane is expected to occur faster than along the c-axis. As a consequence, the growth of anisotropic Sb_2Te_3 hexagons is based on the inherent crystal structure of rhombohedral Sb_2Te_3. Moreover, the nucleation process is expected to be rather fast and the growth process rather slow as is indicated by the formation of uniform nanoplates with narrow size distribution.[64]

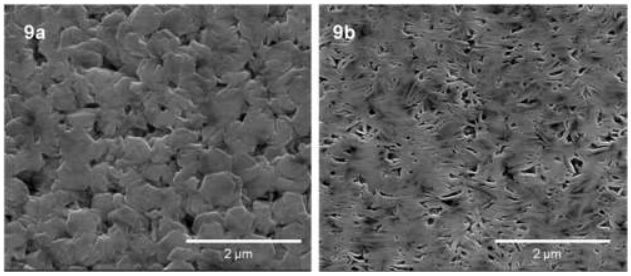

Figure 9. SEM photographs (**9a** top view; **9b** cross-section view) of the "native" cold-pressed Sb_2Te_3 pellet.

In order to demonstrate the potential of the as-prepared nanostructures for thermoelectric application, several cold-pressed pellets were characterized with respect to their thermoelectric properties with and without additional temperature anneal. All transport measurements were done in the pressing direction of the pellets. The cold-pressed pellets had a density of 5.6 g/cm^3 without temperature annealing and 5.75 g/cm^3 with temperature annealing, which corresponds to 85 % and 87 % of the bulk density of Sb_2Te_3, 6.57 g/cm^3. This relatively high porosity and the preferred orientation of the nanoplates perpendicular to the pressing direction of the compaction process is shown by a SEM study of the pellets (Fig. 9). Since the preferred orientation of the nanoplates is perpendicular to the pressing direction, we tentatively correlate this transport direction with the crystallographic c-axis. Figure 10 shows the thermoelectric transport of the 'native' and the annealed powder.

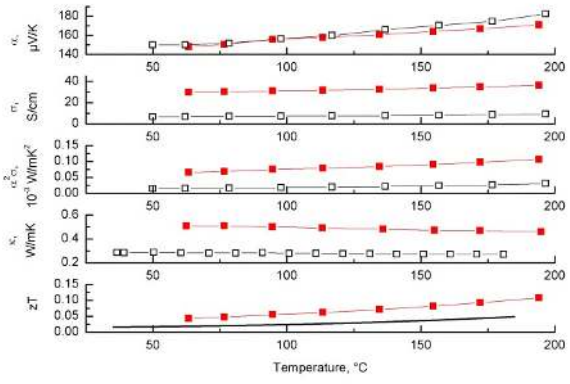

Figure 10. Thermoelectric transport characterization of cold-pressed nanoplates in the temperature range between 25 °C and 200 °C; A 'native' sample, cold-pressed pellets without any temperature annealing (black open squares), and a powder exposed to a rapid thermal annealing (RTA; red filled squares) are shown. The RTA-sample was repeatedly measured. Here, the 3rd run is displayed.

The Seebeck coefficient α has values between 145 µV/K and 170 µV/K which are highly comparable for all measurements, independent on the rapid thermal annealing and repeated measurements. The positive sign of the thermopower clearly demonstrates an intrinsic p-type doping of the material. With respect to the thermoelectric properties, the Seebeck coefficient is the only coefficient solely dependent on material's chemistry, i.e. the electrochemical potential. Hence, the high values of the Seebeck coefficient do not have their origin in the size or shape of the nanoplatelets. They rather originate from the specific defect chemistry of the material and are a result of a slightly under-stoichiometric tellurium concentration, which corresponds very well with the EDX results. The under-stoichiometric tellurium concentration results in the formation of Sb-antisite defects, doping the material. Single crystalline Sb_2Te_3 reference material obtained by travelling heater method has smaller values of the Seebeck coefficient than the ones measured in this study, in the range between around 80 µV/K to 90 µV/K.[65] The reason is that the regulation of the electronically active antisite defect concentration is difficult in Sb_2Te_3. Recently it was reported that a sulphur doping favorably changes the material's chemistry towards a lower Sb-antisite defect concentration and therewith technically relevant values of the Seebeck coefficient.[66] While sulphur defects can be excluded for the here-applied synthesis, this study emphasizes the need of precisely controlling the defect chemistry of Sb_2Te_3 during the synthesis, and it is a strong benefit of the presented *single-source precursor* route that the stoichiometry of the material is high, without the need of further additives like sulphur. Similarly high Seebeck coefficients were recently demonstrated for electrochemically deposited Sb_2Te_3 films.[67]

While the Seebeck coefficients already are in a very favorable range pointing towards ideal composition and defect chemistry of the nanoplates, the relatively low value of the specific electrical conductivity σ demonstrates the need for further optimization of the compaction process. For the 'native' sample the electrical conductivity increases from 6 to 9 S/cm, for the annealed powder from 30 to 36 S/cm. The fact that σ increases with temperature may be an indication for hopping processes which dominate the transport. Since the Seebeck coefficient remained constant even after the annealing but the electrical conductivity improved considerably, it can be concluded that the annealing did not activate additional charge carriers but rather improved the electrical mobility and thus the interfaces between the nanoparticles. Typically, an ideal thermoelectric material should have a density close to 100 % of the bulk density, mainly because the electrical mobility suffers from porosity. In the Sb_2Te_3 system, optimized zT values around 0.7 were reported for cold-pressed and sintered nanoplates from a microwave assisted synthesis procedure with density values in the range of 92 %.[66] The thermal conductivity κ shows very low values, ranging only from 0.29 to 0.27 W/(m·K) for the 'native' sample, whereas 0.51 to 0.46 W/(m·K) were obtained from the annealed powder after three measurement runs. Single crystalline Sb_2Te_3 has a thermal conductivity of 1.6 W/(m·K) along the c-axis at room temperature.[58] Thus, the thermal conductivity

was reduced considerably which may be attributed to both, the nanostructuring approach and the high porosity of the pellets. Optimized Sb_2Te_3 pellets from nanoplates showed values of the total thermal conductivity around 1.36 W/(m·K).[66] Applying the Wiedemann-Franz law, $\kappa_e = L \sigma T$, with $L = 1.66 \times 10^{-8}$ W/(ΩK^2) for Sb_2Te_3,[64] and $\kappa = \kappa_e + \kappa_L$, electronic and phononic contributions to the heat transport can be separated. The lattice thermal conductivity κ_L of the native material is between 0.28 to 0.26 W/(m·K). κ_L of the annealed powder is between 0.48 and 0.42 W/(m·K) in the measured temperature range. Optimized pellets from ref. 66 had 0.35 W/(m·K) lattice thermal conductivity. This small value of κ_L demonstrated by Metha et al. (65) was partly attributed to the sulphur doping, partly to the dominance of the temperature independent phonon scattering at nanograin boundaries and nanopores. Since sulphur contamination can be excluded, the low thermal conductivity of our samples is attributed to scattering at grain boundaries and pores.

The over-all figure of merit zT was 0.08 at 180 °C for the 'native' sample and 0.11 at 195 °C for the annealed powder, but without optimized electronic properties. Future steps in optimizing the material may therefore be an optimization of the compaction and annealing process.

Conclusion. Highly crystalline, nearly monodisperse hexagonal Sb_2Te_3 nanoplates with a thickness of 35 nm were obtained from a controlled thermolysis reaction of the novel *single source precursor* $(Et_2Sb)_2Te$ in the presence of PVP* as size- and shape-controlling agent at 170 °C. PVP* was found to be essential for the stabilization of colloidal-dissolved Sb_2Te_3 nanoplates. The thermoelectric characterization of a cold pressed pellet shows that the Seebeck coefficients of the Sb_2Te_3 nanoplates were in a very favorable regime around 150 µV/K at ambient temperature. This indicates that the controlled thermolysis reaction of the *single source precursor* yields a very low antisite defect concentration and therewith ideal preconditions for thermoelectricity.

AUTHOR INFORMATION

Corresponding Author

* To whom correspondence should be addressed. E-Mail: stephan.schulz@uni-due.de

Author Contributions

All authors have given approval to the final version of the manuscript.

ACKNOWLEDGMENT

Stephan Schulz and Gabi Schierning gratefully acknowledge financial support by the University of Duisburg-Essen.

ABBREVIATIONS

CTAB, hexadecyltrimethylammonium bromide; DIPP, 2,6-diisoporopyl benzene; DSC, differential scanning calorimetry; EDX, energy-dispersive X-ray spectroscopy; TEM, transmission electron microscopy; PVP*, poly(1-vinylpyrolidone)-graft-(1-triacontene), SAED, selected area electron diffraction; SEM, scanning electron microscopy; TOPO, tri-n-octylphosphaneoxid; XRD, X-ray diffraction.

REFERENCES

(1) Xia, Y. N.; Yang, P. D.; Sun, Y. G.; Wu, Y. Y.; Mayers, B.; Gates, B.; Yin, Y. D.; Kim, F.; Yan, Y. Q. *Adv. Mater*. **2003**, *15*, 353.

(2) Kuang, D. B.; Xu, A. W.; Fang, Y. P.; Liu, H. Q.; Frommen, C.; Fenske, D. *Adv. Mater.* **2003**, *15*, 1747.

(3). Fahlman, B. D. *Materials Chemistry*, Vol. 1, Springer, Mount Pleasant, **2007**, pp. 282 – 283.

(4) Halperin, W. P. *Rev. Mod. Phys.* **1986**, *58*, 533.

(5) Kreibig, U.; Vollmer, M. *Optical Properties of Metal Clusters*, Springer, New York, **1995**.

(6) Cui, Y.; Lieber, C. M. *Science* **2001**, *291*, 851.

(7) Kong, J.; Franklin, N. R.; Zhou, C. W.; Chapline, M. G.; Peng, S.; Cho, K. J.; Dai, H. J. *Science* **2000**, *287*, 622.

(8) Xia, Y.; Xiong, Y.; Lim, B.; Skrabalak S. E. *Angew. Chem. Int. Ed.* **2009**, *48*, 60.

(9) Duan, X. F.; Huang, Y.; Cui, Y.; Wang, J. F.; Lieber, C. M. *Nature* **2001**, *409*, 66.

(10) Xia, Y. N.; Yang, P. D.; Sun, Y. G.; Wu, Y. Y.; Mayers, B.; Gates, B.; Yin, Y. D.; Kim, F.; Yan, Y. Q. *Adv. Mater.* **2003**, *15*, 353.

(11) Peng, X. G. *Adv. Mater.* **2003**, *15*, 459.

(12) Pacholski, C.; Kornowski, A.; Weller, H. *Angew. Chem. Int. Ed.* **2002**, *41*, 1188.

(13) Tang, Z.; Kotov, N. A.; Giersig, M. *Science* **2002**, *297*, 237.

(14) Hicks, L. D.; Dresselhaus, M. S. *Phys. Rev. B* **1993**, *47*, 12727.

(15) Hicks, L. D.; Dresselhaus, M. S. *Phys. Rev. B* **1993**, *47*, 16631.

(16) Harman, T. C.; Taylor, P. J.; Spears, D. L.; Walsh, M. P. *J. Electron. Mater.* **2000**, *29*, L1.

(17) Hicks, L. D.; Sun, T. C.; Harman, X.; Dresselhaus, M. S. *Phys. Rev. B* **1996**, *53*, R10493.

(18) Prieto, A. L.; Sander, M. S.; Martin, M. S.; Gronsky, R.; Sands, T.; Stacy, A. M. *J. Am. Chem. Soc.* **2001**, *123*, 7160.

(19) Jin, C. G.; Xiang,X. Q.; Jia, C.; Liu, W. F.; Cai,W. L.; Yao, L. Z.; Li, X. G. *J. Phys. Chem. B* **2004**, *108*, 1844.

(20) Toprak, M.; Zhang, Y.; Muhammed, M. *Mater. Lett.* **2003**, *57*, 3976.

(21) Yu, S. H.; Yang, J.; Wu, Y. S.; Han, Z. H.; Lu, J.; Xie, Y.; Qian, Y. T. *J. Mater. Chem.* **1998**, *8*, 1949.

(22) Wang, W. Z.; Poudel, B.; Wang, D. Z.; Ren, Z. F. *Adv. Mater.* **2005**, *17*, 2110.

(23) Wang, W. Z.; Poudel, B.; Yang, J.; Wang, D. Z.; Ren, Z. F. *J. Am. Chem. Soc.* **2005**, *127*, 13792.

(24) Zhang, H. T.; Luo, X. G.; Wang, C. H.; Xiong, Y. M.; Li, S. Y.; Chen, X. H. *J. Cryst. Growth* **2004**, *265*, 558.

(25) Venkatasubramanian, R.; Siivola, E.; Colpitts, T.; O'Quinn, B. *Nature* **2001**, *413*, 597.

(26) Harman, T. C.; Taylor, P. J.; Walsh, M. P.; LaForge, B. E. *Science* **2002**, *297*, 2229.

(27) Christian, P.; O'Brien, P. *J. Mater. Chem.* **2005**, *15*, 4949.

(28) Zou, H.; Rowe, D. M.; Min, J. *J. Vac. Sci. Technol. A* **2001**, *19*, 899.

(29) ElMandouh, Z. S. *J. Mater. Sci.* **1995**, *30*, 1273.

(30) Das, V. D.; Soundararajan, N.; Pattabi, M. *J. Mater. Sci.* **1987**, *22*, 3522.

(31) Dresselhaus, M. S.; Chen, G.; Tang, M. Y.; Yang, R. G.; Lee, H.; Wang, D. Z.; Ren, Z. F.; Fleurial, J. P.; Gogna, P. *Adv. Mater.* **2007**, *19*, 1043.

(32) Yan, Q. Y.; Chen, H.; Zhou, W. W.; Hng, H. H.; Boey, F. Y. C.; Ma, J. *Chem. Mater.* **2008**, *20*, 6298.

(33) Wang, R. Y.; Feser, J. P.; Lee, J. S.; Talapin,D. V.; Segalman, R.; Majumdar, A. *Nano Lett.* **2008**, *8*, 2283.

(34) Poudel, B.; Hao, Q.; Ma, Y.; Lan, Y. C.; Minnich, A.; Yu, B.; Yan, X.; Wang, D. Z.; Muto, A.; Vashaee, D.; Chen, X. Y.; Liu, J. M.; Dresselhaus,M. S.; Chen, G.; Ren, Z. *Science* **2008**, *320*, 634.

(35) Hsu, K. F.; Loo, S.; Guo, F.; Chen, W.; Dyck, J. S.; Uher, C.; Hogan, T.; Polychroniadis, E. K.; Kanatzidis, M. G. *Science* **2004**, *303*, 818.

(36) Hochbaum, A. I.; Chen, R. K.; Delgado, R. D.; Liang, W. J.; Garnett, E. C.; Najarian, M.; Majumdar, A.; Yang, P. D. *Nature* **2008**, *451*, 163.

(37) Meister, S.; Peng, H. L.; McIlwrath, K.; Jarausch, K.; Zhang, X. F.; Cui, Y. *Nano Lett.* **2006**, *6*, 1514.

(38) Lee, J. S.; Brittman, S.; Yu, D.; Park, H. *J. Am. Chem. Soc.* **2008**, *130*, 6252.

(39) Garje, S. S.; Eisler, D. J.; Ritch, J. S.; Afzaal, M.; O'Brien P.; Chivers, T. *J. Am. Chem. Soc.* **2006**, *128*, 3120.

(40) Chen, J.; Sun, T.; Sim, D. H.; Peng, H.; Wang, H.; Fan, S.; Hng, H. H.; Ma, J.; Boey, F. Y. C.; Li, S.; Samani, M. K.; Chen, G. C. K.; Chen, X.; Wu, T.; Yan Q. *Chem. Mater.* **2010**, *22*, 3086.

(41) Wang, Q.; Jiang, C. L.; Yu C. F.; Chen, Q. W. *J. Nanopart. Res.* **2007**, *9*, 269.

(42) Shi, W. D.; Yu, J. B.; Wang, H. S.; Zhang, H. J. *J. Am. Chem. Soc.* **2006**, *128*, 16490.

(43) Wang, Z. W.; Yan, X.; Poudel, B.; Ma, Y.; Hao, Q.; Yang, J.; Chen, G.; Ren, Z. F. *J. Nanosci. Nanotechnol.* **2008**, *8*, 452.

(44) Shi, S.; Cao, M.; Hu, C. *Cryst. Growth Des.* **2009**, *9*, 2057.

(45) Zhang, G. Q.; Wang, W.; Lu, X. L.; Li, X. G. *Cryst. Growth Des.* **2009**, *9*, 145.

(46) Yuan, Q. L.; Nie, Q. L.; Huo, D. X. *Curr. Appl. Phys.* **2009**, *9*, 224.

(47) Zhou, B.; Ji, Y.; Yang, Y. F.; Li X. H.; Zhu, J. H. *Cryst. Growth Des.* **2008**, *8*, 4394.

(48) Shi, W.; Zhou, L.; Song, S.; Yang, J.; Zhang, H. *Adv. Mater.* **2008**, *20*, 1892.

(49) Drasar, C.; Steinhart, M.; Lostak, P.; Shin, H. K.; Dyck, J. S.;Uher, C. J. *Solid State Chem.* **2005**, *178*, 1301.

(50) Dhar, S. N.; Desai, C. F. *Philos. Mag. Lett.* **2002**, *82*, 581.

(51) Zhang, Y.; Snedaker, M. L.; Birkel, C. S.; Mubeen, S.; Ji, X.; Shi, Y.; Liu, D.; Liu, X.; Moskovits, M.; Stucky, G. D. *Nano Lett.* **2012**, *12*, 1075.

(52) Meinema, H. A.; Martens, H. F.; Noltes, J. G. *J. Organomet. Chem.* **1973**, *51*, 223.

(53) Breunig, H. J.; Jawad, H. *J. Organomet. Chem.* **1984**, *277*, 257.

(54) Pashinkin, A. S.; Malkova, A. S.; Mikhailova, M. S. *Russ. J. Phys. Chem.* **2008**, *82A*, 878.

(55) Haaland, A.; Shorokhov, D. J.; Sokolov, V. I.; Volden, H. V.; Breunig, H. J.; Denker, M.; Rösler, R. *Phosphorur, Sulfur Silicon Relat. Elem.* **1998**, *136, 137 & 138*, 463.

(56) Haaland, A.; Shorokhov, D. J.; Volden, H. V.; Breunig, H. J.; Denker, M.; Rösler, R. *Z. Naturforsch.* **1998**, *53b*, 381.

(57) Speight, J. G. ***Lange's Handbook of Chemistry***; 16th ed., McGraw-Hill, New York, 2005, Section 1, p 22.

(58) Garje, S. S.; Eisler, D. J.; Ritch, J. S.; Afzaal, M.; O'Brien, P.; Chivers, T. *J. Am. Chem. Soc.* **2006**, *128*, 3120.

(59) Wang, W.; Long, D.; Liang, Y.; Zhang, G.; Zeng, B.; He, Q. *Langmuir* **2011**, *27*, 815.

(60) Zhang, H. Wang, H. Xu, Y. Zhuo, S. Yu, Y., Zhang, B. *Angew. Chem. Int. Ed.* **2012**, *51*, 1459.

(61) Jin, R.; Chen, G.; Pei, J.; Xu, H.; Lv Z. S. *RSC Adv.* **2012**, *2*, 1450.

(62) Lu, W.; Ding, Y.; Chen, Y.; Wang, Z. L.; Fang, J. *J. Am. Chem. Soc.* **2005**, *127*, 10112.

(63) Hollingsworth, J. A.; Poojary, D. M.; Clearfield, A.; Buhro, W. E. *J. Am. Chem. Soc.* **2000**, *122*, 3562.

(64) Cushing, B. L. Kolesnichenko, V. L. O'Connor, C. J. *Chem. Rev.* **2004**, *104*, 3893.

(65) Scherrer, H; Scherrer, S. *Thermoelectrics Handbook, Macro to Nano*, Ed. D.M. Rowe, Francis & Taylor group, Boca Raton, Florida, 2006, Chapter 27.

(66) Mehta, R. J.; Zhang, Y.; Karthik, C.; Singh, B.; Siegel, R. W.; Borca-Tasciuc, T.; Ramanath, G. *Nature Mater.* **2012**, *11*, 233.

(67) Schumacher, C.; Reinsberg, K. G.; Akinsinde, L.; Zastrow, S.; Heiderich, S.; Toellner, W.; Rampelberg, G.; Detavernier, C.; Broekaert, J. A. C.; Nielsch, K.; Bachmann, J. *Adv. Energy Mater.* **2012**, *2*, 345.

DOI: 10.1021/cm301259u
URN: urn:nbn:de:hbz:464-20201112-092806-3

This document is the **Accepted Manuscript** version of a Published Work that appeared in final form in: Chem. Mater. 2012, 24, 11, 2228–2234, copyright © American Chemical Society after peer review and technical editing by the publisher.
To access the final edited and published work see: https://doi.org/10.1021/cm301259u